

See discussions, stats, and author profiles for this publication at: <https://www.researchgate.net/publication/5577272>

Solid-State Deuterium NMR Studies Reveal μ s–ns Motions in the HIV-1 Transactivation Response RNA Recognition Site

ARTICLE *in* JOURNAL OF THE AMERICAN CHEMICAL SOCIETY · APRIL 2008

Impact Factor: 12.11 · DOI: 10.1021/ja0778803 · Source: PubMed

CITATIONS

32

READS

19

6 AUTHORS, INCLUDING:



Greg L Olsen

Weizmann Institute of Science

15 PUBLICATIONS 263 CITATIONS

SEE PROFILE



Dorothy Echodu

Pilgrim Africa

7 PUBLICATIONS 119 CITATIONS

SEE PROFILE



Zahra Shajani Yi

Dartmouth–Hitchcock Medical Center

18 PUBLICATIONS 526 CITATIONS

SEE PROFILE



Michael F. Bardaro

University of Washington Seattle

12 PUBLICATIONS 149 CITATIONS

SEE PROFILE

Published in final edited form as:

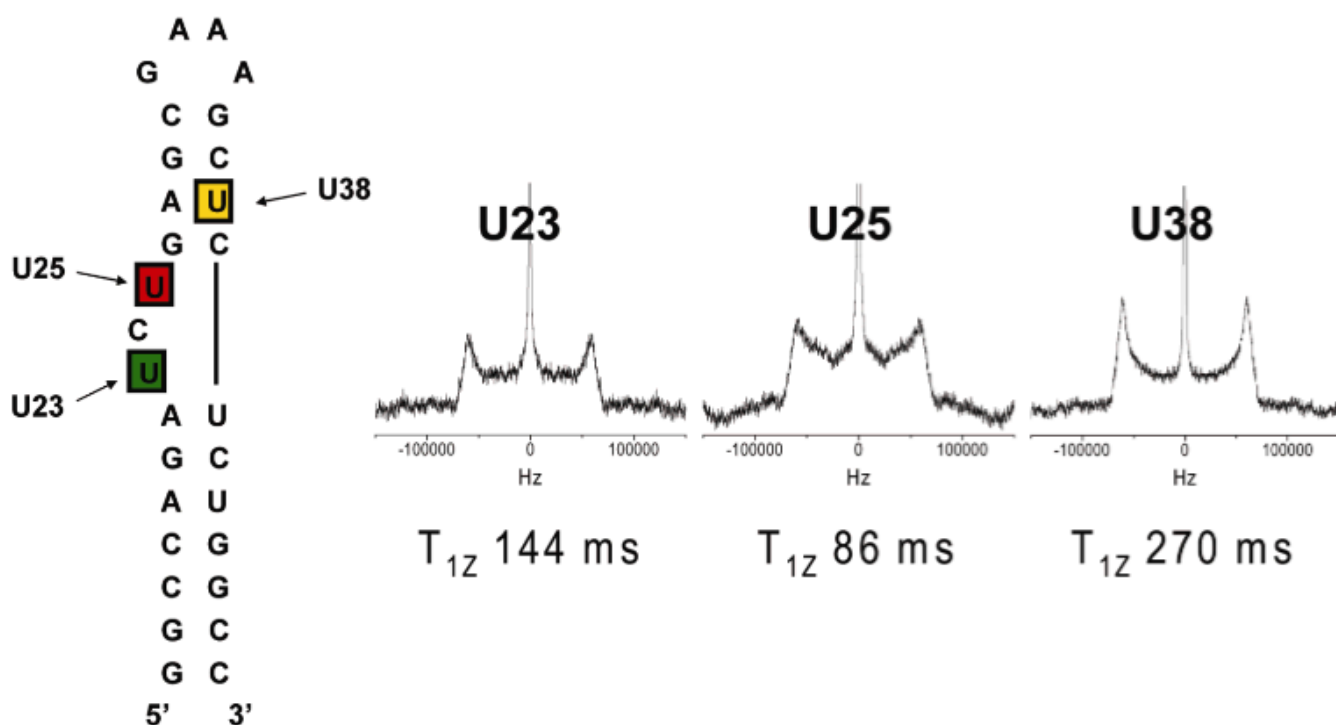
J Am Chem Soc. 2008 March 12; 130(10): 2896–2897. doi:10.1021/ja0778803.

Solid-State Deuterium NMR Studies Reveal μ s-ns Motions in the HIV-1 TAR RNA Recognition Site

Greg L. Olsen, Dorothy C. Echodu, Zahra Shajani, Michael F. Bardaro Jr., Gabriele Varani, and Gary P. Drobny

Departments of Chemistry and Biochemistry, University of Washington, Seattle, Washington, 98195

Abstract



Solution and solid-state NMR measurements were used together to examine motion in three sites in the HIV-1 TAR RNA. We wished to investigate the dynamics facilitating the conformational rearrangements the TAR RNA must undergo for tat binding, and in particular to characterize the full range of motional timescales accessible to this RNA. Our results demonstrate that the dynamics in TAR involving residues essential to tat binding include not only the faster motions detected by solution relaxation measurements, but also a significant component in the μ s-ns timescale.

The HIV-1 transactivation response (TAR) RNA provides a classic example of adaptive protein-RNA recognition^{1,2} and is of key importance for viral replication. Transcription of the HIV genome is dependent upon binding of the viral regulatory protein tat at a three-nucleotide bulge linking two short helices comprising the TAR hairpin³ (Figure 1). The inherent flexibility of this bulge allows it to undergo a conformational transition upon binding of Tat protein or

even of a single arginine, generating the structure required to form a specific protein-RNA complex^{1,2}. The structures of the free RNA and of the Tat- or arginine-bound RNA are known; how the RNA traverses the intervening conformational landscape is not. In order to understand how TAR functions, it is necessary to characterize the full range of motions accessible to this RNA. Such knowledge would provide mechanistic insight into how the conformational changes occur and how the dynamics information required for tat binding is encoded in the TAR sequence.

Solution NMR studies have begun to uncover complex dynamics in many RNAs, revealing rich local and collective dynamics in the ps-ns and μ s-ms timescales⁵⁻¹². However, solution NMR methods fail to capture motions that occur in the μ s-ns timescale. In contrast to solution relaxation methods, deuterium solid-state NMR lineshape measurements are particularly sensitive to motions in the μ s-ns range. We recently observed extensive motions within this dynamic window in the DNA target of a methyltransferase using solid-state NMR¹³, and wished to investigate whether TAR RNA was dynamically rich within the μ s-ns timescale as well as in the faster and slower regimes.

Previous ²H solid-state NMR investigations of RNA dynamics have studied uniformly C8-labeled duplex samples, precluding delineation of the motional properties of individual residues¹⁴⁻¹⁶. Here we report the first site-specific ²H solid-state NMR study of RNA. The solid-state experiments were used to probe three sites with different structural characteristics^{3,6}. U23 and U25 are both single-stranded, but while U23 is stacked on a neighboring base, while U25 is neither base-paired nor stacked. U38 is part of a base-paired helix; U23 and U38 are critical for TAR function (Figure 1a). Quadrupole echo lineshape and $T_{1\rho}$ relaxation data were collected for 5,6-²H uridine nucleobase labels introduced at these three positions in separate 29-nucleotide TAR constructs. Each RNA sample was hydrated to 16 waters per nucleotide, to reproduce conditions under which nucleic acid motions have been shown to be similar to those observed in solution¹⁶⁻¹⁸. Under these conditions, local hydration of the nucleic acid backbone and bases is substantially complete so that local dynamics are essentially solution-like; introduction of additional waters only adds to bulk hydration, facilitating global tumbling and negating the advantages of the solid-state investigation.

Motions occurring at rates in the 10⁶-10⁹ Hz range modulate the quadrupolar lineshape²⁰. The deuterium lineshape is thus especially useful in revealing dynamics too slow to be detected by solution relaxation measurements (ns-ps) or too fast to be detected by rotating frame relaxation measurements (ms- μ s). Motions occurring at rates greater than the Larmor frequency “pre-average” the electric field gradient tensor and effectively scale the width of the deuterium spectrum. The effects of these motions can be expressed in terms of order parameters. For rates slower than the Larmor frequency ($\nu_0 \sim 10^8$ Hz), but faster than the quadrupolar coupling constant ($\nu_Q = e^2qQ/h; \sim 1.7 \times 10^5$ Hz for the present work), the modulation of the powder pattern is more complex²¹. However, deviation from a static Pake powder pattern - often visible as trajectory-dependent spectral averaging between the ‘horns’ of the powder pattern - is diagnostic for motions on this timescale (Figure 2).

The ²H solid-state NMR lineshapes from TAR reveal the presence of distinct dynamics at each of the three sites (Figure 2). U38 retains the features of a Pake doublet, similar to lineshapes observed previously for bases in double-stranded DNA devoid of significant internal motions²²⁻²³. In contrast, both U23 and U25 clearly show lineshape modulations indicative of motion on the intermediate spectral timescale. Consistent with the presence of distinct motions at these three sites, the Zeeman spin-lattice relaxation time ($T_{1\rho}$) was 270 ms for U38, but was considerably shorter for U23 and U25 (144 and 86 ms, respectively).

In order to compare the dynamics observed by solid-state NMR with what is observed in solution, we also measured ^{13}C solution NMR relaxation rates for C6/C8 and C1' sites throughout TAR, including the three sites probed in the solid-state experiments described above. While U25 was not sufficiently resolved from other resonances in the spectrum of TAR to enable measurement of its relaxation properties, results were obtained for U23 and U38. Data were analyzed using the model-free approximation, to determine in particular whether slower motions or conformational exchange (R_{ex}) were present, and to establish the degree of spatial restriction (S^2) at these sites. The base (C6) data for U38 in these experiments (Table 1) are indicative of restricted motions consistent with a rigid helical residue (lower heteronuclear NOE and high S^2 order parameter), and are thus in good agreement with the solid-state data and previous ^2H relaxation measurements in solution²⁴. The shorter C6 T_I seen for U23, in combination with the relatively large $T_{I\pi}$ and NOE values observed here, suggests the presence of ps-ns base motion at this position. Intriguingly, the C1' solution NMR data suggest that the sugar-phosphate backbone at U23 is less restricted than the base itself in the free RNA, as was also observed by deuterium solution NMR²⁴. Notably, R_{ex} values for C6 and C1' as determined from the model-free analysis at both positions were negligibly small, suggesting the absence of slower (ms- μs) base and furanose motions at these sites, in agreement with previous work^{6, 25}.

The solid-state results demonstrate that TAR RNA dynamics involving residues essential to tat binding include not just the faster timescale motions probed by solution relaxation measurements, but also a significant component in the μs -ns timescale. Motion in the μs -ns regime is clearly apparent in the strongly modulated ^2H powder patterns for both U23 and U25; the trend in relaxation times, $T_{I\text{Z}}(\text{U38}) > T_{I\text{Z}}(\text{U23}) > T_{I\text{Z}}(\text{U25})$, indicates progressively greater dynamics near the ^2H Larmor frequency, from the rigid helical environment of U38 to the partially stacked environment of U23 to the relatively unconstrained environment of U25. These motions were not observed in solution relaxation measurements, as they were not fast enough to affect relaxation parameters nor slow enough to modulate solution lineshapes. However, they may have been responsible for the reported discrepancy between order parameters calculated from solution relaxation or from residual dipolar couplings (RDC's)²⁷. Smaller order parameters for RDC's probably reflected additional motions that averaged their values yet did not affect the relaxation rates, as we report here. The slower motions we detect may also be connected to the inter-helical motions observed by domain elongation¹¹.

To our knowledge, this work represents the first site-specific ^2H solid-state NMR study of RNA dynamics. Given the importance of understanding the functional roles of dynamics in RNA, and the demonstrated presence of motions in ranges accessible either to solution or solid-state measurements - but not to both methods - the parallel application of solid-state and solution NMR methods will be necessary to construct a complete picture of the motions present in TAR and other RNAs. Our results in both DNA and RNA also suggest that this generally overlooked dynamic window (μs -ns) may be equally rich in proteins as it clearly is in nucleic acids.

Supplementary Material

Refer to Web version on PubMed Central for supplementary material.

Acknowledgments

This research was supported by NIH RO1 EB0315 and NSF MCB 0642253.

References

- (1). Puglisi JD, Tan R, Calnan BJ, Frankel AD, Williamson JR. *Science* 1992;257:76–80. [PubMed: 1621097]
- (2). Aboul-Ela F, Karn J, Varani G. *J. Mol. Biol* 1995;253:313–332. [PubMed: 7563092]
- (3). Karn J. *J. Mol. Biol* 1999;293:235–254. [PubMed: 10550206]
- (4). Aboul-Ela F, Karn J, Varani G. *Nucl. Acids Res* 1996;24:3974–3981. [PubMed: 8918800]
- (5). Hoogstraten CG, Wank JR, Pardi A. *Biochemistry* 2000;39:9951–9958. [PubMed: 10933815]
- (6). Dayie KT, Brodsky AS, Williamson JR. *J. Mol. Biol* 2002;317:263–278. [PubMed: 11902842]
- (7). Al-Hashimi HM, Gosser Y, Gorin A, Hu W, Mujamdar A, Patel DJ. *J. Mol. Biol* 2002;315:95–102. [PubMed: 11779230]
- (8). Shajani Z, Varani G. *J. Mol. Biol* 2005;399:699–715. [PubMed: 15890361]
- (9). Blad H, Reiter NN, Abildgaard F, Markley JL, Butcher SE. *J. Mol. Biol* 2005;353:540–555. [PubMed: 16181635]
- (10). Duchardt E, Schwalbe H. *J. Biomol. NMR* 2005;32:295–308. [PubMed: 16211483]
- (11). Zhang Q, Sun X, Watt ED, Al-Hashimi HM. *Science* 2006;311:653–656. [PubMed: 16456078]
- (12). Shajani Z, Varani G. *Biopolymers* 2007;86:348–359. [PubMed: 17154290]
- (13). Miller P, Shajani Z, Meints GA, Caplow D, Goobes G, Varani G, Drobny GP. *J. Am. Chem. Soc* 2006;128:15970–15971. [PubMed: 17165714]
- (14). Wang AC, Kennedy MA, Reid BR, Drobny GP. *J. Am. Chem. Soc* 1992;114:6583–6585.
- (15). Tsang P, Kearns DR, Vold RR. *J. Am. Chem. Soc* 1992;114:6585–6587.
- (16). Wang AC, Kennedy MA, Reid BR, Drobny GP. *J. Magn. Res* 1994;105:1–10.
- (17). Falk M, Hartman KA, Lord RC. *J. Am. Chem. Soc* 1962;84:3843–3846.
- (18). Schurr JM, Fujimoto BS, Diaz R, Robinson BH. *J. Magn. Res* 1999;140:404–431.
- (19). Greenfield MS, Ronemus AD, Vold RL, Vold RR, Ellis PD, Raidy TE. *J. Mag. Res* 1987;72:89–107.
- (20). Spiess HW, Sillescu H. *J. Magn. Res* 1981;42:381–389.
- (21). Abragam, A. *The Principles of Nuclear Magnetism*. Clarendon Press; Oxford, England: 1961.
- (22). Kintnar A, Huang W-C, Schindele DC, Wemmer DE, Drobny G. *Biochemistry* 1989;28:282–293. [PubMed: 2706252]
- (23). Brandes R, Vold RR, Vold RL, Kearns DR. *Biochemistry* 1986;25:7744–7751. [PubMed: 3026460]
- (24). Vallurupalli P, Scott L, Hennig M, Williamson JR, Kay LE. *J. Am. Chem. Soc* 2006;128:9346–9347. [PubMed: 16848466]
- (25). Vallurupalli P, Scott L, Williamson JR, Kay LE. *J. Biomol. NMR* 2007;38:41–46. [PubMed: 17334825]
- (26). Getz M, Sun X, Casiano-Negroni A, Zhang Q, Al-Hashimi HM. *Biopolymers* 2007;86:384–402. [PubMed: 17594140]

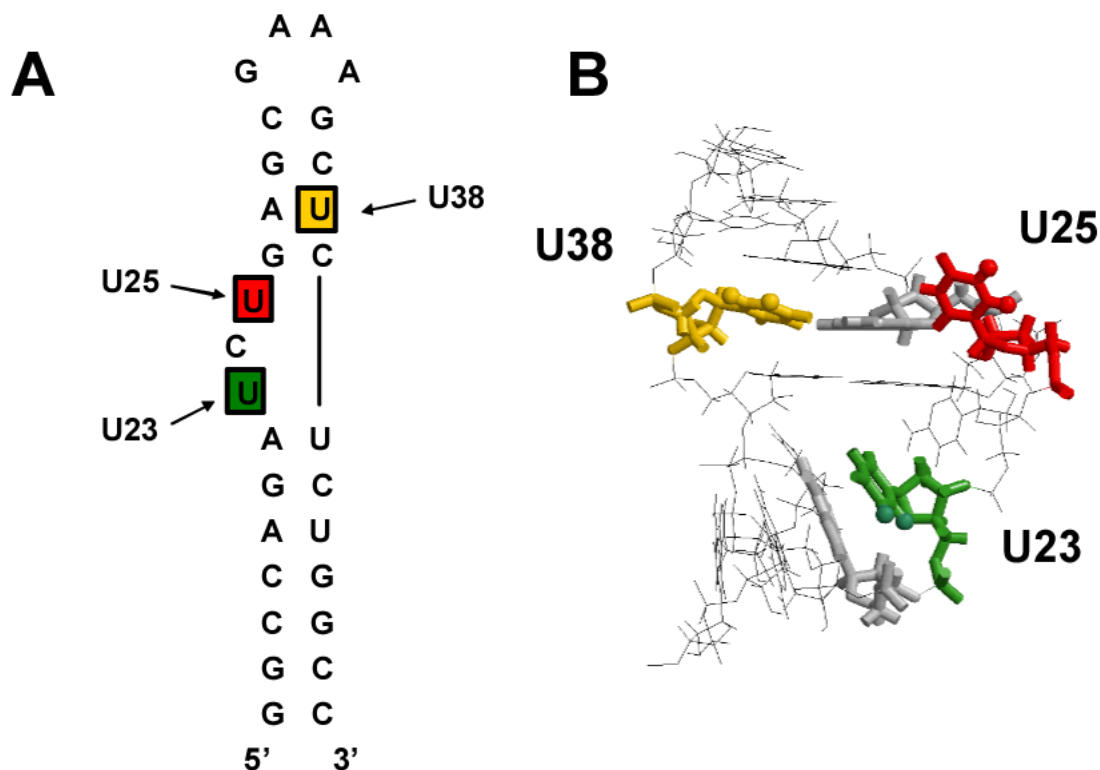


Figure 1.

a) Secondary structure of HIV-1 TAR RNA, showing the three sites where 5,6-²H deuterium labels were introduced for solid-state NMR studies. b) Close-up view of the structure of unbound TAR⁴, showing the different structural contexts of the three nucleotides studied here. Colored spheres denote 5,6-²H nucleobase label positions. U23 (green) is single-stranded, but stacked on the adjacent base (A22, in grey); U25 (red) is largely disordered; U38 (yellow) is base paired with A27 (in grey) and part of a canonical Watson-Crick paired helix. U23 and U38 play critical roles in binding of Tat protein; U25 functions as a spacer^{1,2}.

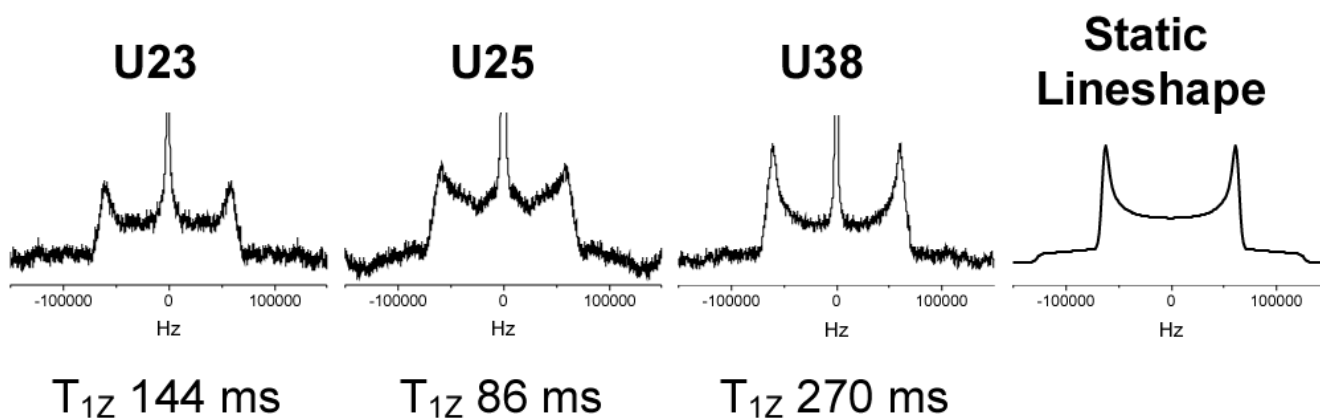


Figure 2.

Deuterium solid-state NMR spectra and corresponding Zeeman spin-lattice (T_{1Z}) relaxation times for 5,6- ^2H labels at positions U23, U25, and U38 in TAR RNA, with a static reference lineshape simulated using MXET1¹⁹. Spectra were acquired at room temperature; all samples were hydrated to 16 waters per nucleotide to ensure conditions similar to those observed in solution¹⁶⁻¹⁸ (see Supplementary material). The narrow central isotropic component in the experimental spectra is due to residual deuterium in the water of hydration.

Table 1

^{13}C solution NMR relaxation data and corresponding ModelFree order parameters for C6 and C1' sites in TAR residues U38 and U23; all relaxation times are in milliseconds. Average C6 relaxation rates for double-helical residues were 355 ms (T_1); 25 ms ($T_{1\rho}$); 1.16 (NOE); and 0.96 (S^2). Average double-helical C1' values were 534 ms (T_1); 37 ms ($T_{1\rho}$); 1.23 (NOE); and 0.93 (S^2)

	U38 - C6	U23 - C6	U38 - C1'	U23 - C1'
T_1	354	328	497	330
$T_{1\rho}$	26	29	38	49
NOE	1.14	1.32	1.25	1.43
S^2	0.97	0.82	0.95	0.67